Journal of Materials Chemistry A

Accepted Manuscript

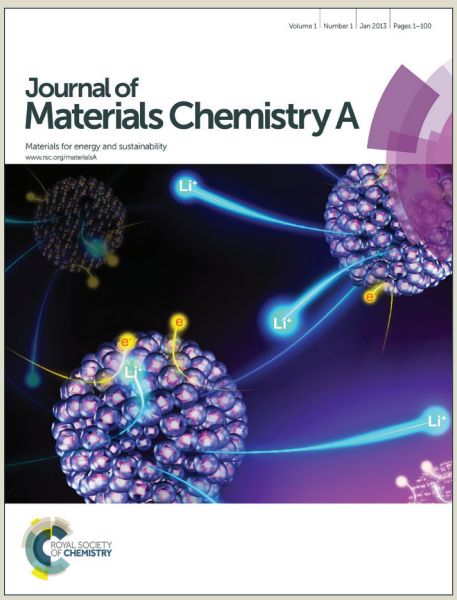

ROYAL SOCIETY OF CHEMISTRY

www.rsc.org/materialsA

Table of Contents

A stable metal-organic framework with suitable pore sizes and rich uncoordinated nitrogen atoms on the internal surface of microspores for highly efficient CO_2 capture

Shao-Juan Bao,[a] Rajamani Krishna,[c] Ya-Bing He,[d] Jun-Sheng Qin,[a] Zhong-Min Su,*[a] Shun-Li Li,[a] Wei Xie,[a] Dong-Ying Du,*[a], Wen-Wen He,[a] Shu-Ran Zhang[a] and Ya-Qian Lan*[a,b]

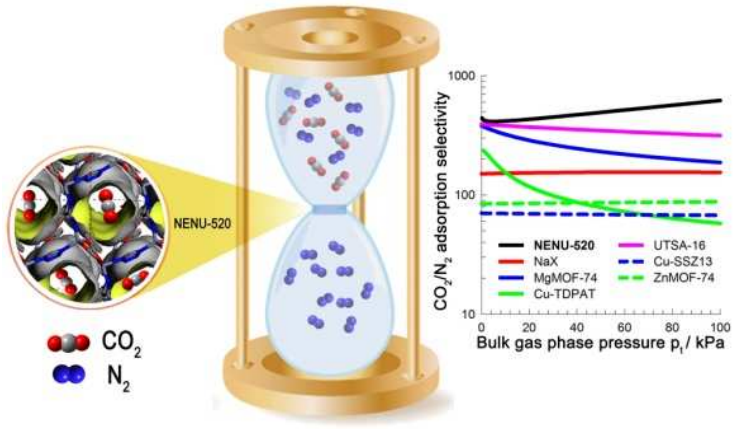

A highly stable tetrazolate-containing framework (**NENU-520**) has been successfully synthesized. **NENU-520** exhibits exceptionally high selectivity of CO_2/N_2 at 298 K.

Journal Name

RSCPublishing

ARTICLE

A stable metal-organic framework with suitable pore sizes and rich uncoordinated nitrogen atoms on the internal surface of microspores for highly efficient CO_2 capture†

Cite this: DOI: 10.1039/xoxxoooooox

Received ooth January 2012,
Accepted ooth January 2012

DOI: 10.1039/xoxxoooooox

www.rsc.org/

Shao-Juan Bao,[a] Rajamani Krishna,[c] Ya-Bing He,[d] Jun-Sheng Qin,[a] Zhong-Min Su,*[a] Shun-Li Li,[a] Wei Xie,[a] Dong-Ying Du,*[a] Wen-Wen He,[a] Shu-Ran Zhang[a] and Ya-Qian Lan*[a,b]

An air-stable tetrazolate-containing framework, $[Zn_2L_2]\cdot 2DMF$ (**NENU-520**, H_2L = 4-(1*H*-tetrazole-5-yl)biphenyl-4-carboxylic acid), with uncoordinated N atoms on the internal surface was solvothermally synthesized and structurally characterized. This metal-organic framework (MOF) exhibited high CO_2 uptakes of 79.9 $cm^3\ cm^{-3}$ at 298 K and 100 kPa, as well as excellent adsorption selectivities of CO_2 over CH_4 and N_2. Particularly, the exceptionally high selectivity of CO_2 over N_2 at 298 K has ranked **NENU-520** among the highest MOFs for selective CO_2 separation. Furthermore, the potential application of **NENU-520** for the fixed bed pressure swing adsorption (PSA) separation of CO_2 from CH_4 and N_2 has been validated *via* simulated breakthrough experiments. The small channel with the size of 3.6 Å, combined with CO_2-accessible free nitrogen atoms directing toward the inner surface, is believed to contribute to the high CO_2 uptake capacity and selectivity. Thus, this work represents a unique way to target MOF materials for the highly selective CO_2 separation by incorporating CO_2-philic functional sites on the pore surfaces, and at the same time optimizing the pore sizes.

Carbon dioxide (CO_2) emissions, which are inevitable, are mainly generated from the anthropogenic combustion of coal, oil and natural gas, the main energy resources for our daily life, economic growth and industrial development.[1-5] With the growing increase of the amount of CO_2 in the atmosphere, the undesirable global warming and climate change have attracted increasing attention.[6-10] Moreover, in addition to its involvement in greenhouse effect, CO_2 is also highly associated with many issues such as separation of CO_2 from industrial gas for bioremediation, demands of selectively capture CO_2 from methane in biogas streams and post-combustion flue gases generated from coal-fired power stations.[11-13] Consequently, there remains an urgent need to selectively capture and sequestrate CO_2 to reduce its negative effect in the atmosphere. Two points must first be made with regards to capture materials and long-term usage. Firstly, they should be highly air-stable and can maintain their stability over multiple cycles for the practical applications as functional materials.[14,15] And secondly, a promising adsorbent for practical applications should possess not only good adsorption capacity but also high selectivity.[16-18] The adsorption capacity depends on the equilibrium pressure and temperature, the nature of the adsorbate, and the nature of the micropores in the adsorbent. While, to a great extent, the selective capture of CO_2 is related to the nature of the adsorbent besides the operational temperature and pressure.

Due to its high surface areas, high void volumes and controlled pore sizes, metal-organic frameworks (MOFs) represent a rapidly expanding, probable new class of porous adsorbents with a large range of possibilities for designing functional materials.[19-22] Focusing on exploiting their high surface areas and large pore size conventionally are far from enough. To date, various feasibility strategies have been explored to enforce their interactions and thus enhance the adsorption capacity and selectivity of MOFs toward CO_2, such as introduction of high density of open metal sites, charged skeleton of MOFs, decoration with polar substituent groups (for instance, $-COOH$, $-NH_2$, $-OH$).[23-27] Moreover, given the fact that the kinetic diameters of the cylinders are 3.3 Å 3.64 Å and 3.80 Å for CO_2, N_2 and CH_4, respectively, size selectivity is attractive characteristics for CO_2 separation and capture.[28,29] To realize effectively separate CO_2 on the basis of size, precise control of the limiting pore diameter is of significant importance. The study of CO_2 selectivity based on small pore size is numbered, albeit more and more MOFs have been reported.

A straightforward approach was put forward and experienced by groups of Chen, Bu, Zhao and Su.[30-33] Introduction of

abundant uncoordinated nitrogen atoms may produce stronger interaction with CO_2. Typically, the interaction between the localized dipoles of the N-containing group and the quadrupole moment of CO_2 would induce the dispersion and electrostatic forces to enhance CO_2 adsorption and separation abilities on MOFs. Nevertheless, high percentage of N-donor sites is not always beneficial to further enhance the interaction with CO_2 molecules. For example, when the lone electron pairs of partially exposed nitrogen atoms do not point into the channels of the frameworks or the uncoordinated N-donor sites be blocked by functionalized groups, they have lower effect on the improvement of CO_2 capacity. It is of crucial importance to construct MOFs that effectively utilize the accessible nitrogen atoms from organic linkers.

Here, we selected a tetrazolate-containing H_2L (4-(1*H*-tetrazole-5-yl)biphenyl-4-carboxylic acid) as organic linker to construct a new MOF. Fortunately, an air-stable zinc-based MOF, $[Zn_2L_2]\cdot 2DMF$ (**NENU-520**, **NENU** = Northeast Normal University) was successfully synthesized and the inner surface is polarized with uncoordinated nitrogen atoms. It features a small channel (3.6 Å, being a little larger than the kinetic diameter of CO_2), which is favourable for its potential application in gas capture and separation. As anticipated, activated sample **NENU-520a** exhibits high uptake of CO_2 and H_2 with high isosteric heat. Selectivities of CO_2/CH_4 and CO_2/N_2 were evaluated using ideal adsorbed solution theory (IAST) and simulated breakthrough experiments. Remarkably, the results from these studies all confirm that the selectivity of CO_2/N_2 has featured **NENU-520** among the highest porous MOF for CO_2 selective separation under ambient conditions. **NENU-520** is one of the best materials to facilitate effective CO_2 separation and capture

Results and discussion

NENU-520 was synthesized by the solvothermal reaction of $Zn(NO_3)_2\cdot 6H_2O$ and H_2L in a mixture solvent of DMF–EtOH with the addition of a small amount of HNO_3 at 90 ℃ for 3 days. The highly crystallized **NENU-520** was formulated as $[Zn_2L_2]\cdot 2DMF$, on the basis of single-crystal X-ray diffraction study. The X-ray crystallographic analysis reveals that **NENU-520** crystallizes in the monoclinic space group *Cc* (Table S1). The asymmetric unit consists of two independent Zn(II) atoms, one coordinated DMF molecule, one DMF solvent and two distinct L^{2-} moieties (Fig. 1a). In **NENU-520**, Zn1 and Zn2 atoms are linked by carboxyl groups to form a binuclear zinc cluster, in addition, each tetrazolyl group bonds two independent Zn atoms from two zinc clusters. In **NENU-520**, each ligand uses just two N atoms for the framework formation, leaving two other open N-donor sites. Such interlinkage generates a 1D smaller-size curving channel running along the *b* axis with a size of ~3.6 Å (Fig. 1b and 1c). The Connolly surface diagram (Fig. 1d) displays the irregular channels of the framework structures. It is obvious that the left two N atoms are point to the inner surface (Fig. 1e). The overall framework can be designated as a (3, 3, 6)-connected network (Fig. S4a) with the point symbol of $(4\ 6^2)_2(4^2\ 6^7\ 8^6)$ analyzed by the TOPOS program, if L^{2-} and binuclear zinc cluster are regarded as 3- and 6-connected nodes, respectively. Further close observation on the structure shows that **NENU-520** can be simplified as a (4, 4)-connected topology with the point symbol of $(4^2\ 6^6\ 8)$, when each Zn atom and L^{2-} fragment is considered as discrete 4-connected node (Fig. S3). And the phase purity of the bulk material was independently confirmed by powder X-ray diffraction (PXRD, Fig. S4b). Upon removing DMF solvent molecules solvent, **NENU-520** forms a microporous framework containing 27.4% solvent void accessible.[34] It is noteworthy that complex **NENU-520** shows good air-stability even exposed in the air for more than two weeks (Fig. S5), which is of the utmost importance for practical application.[35,36]

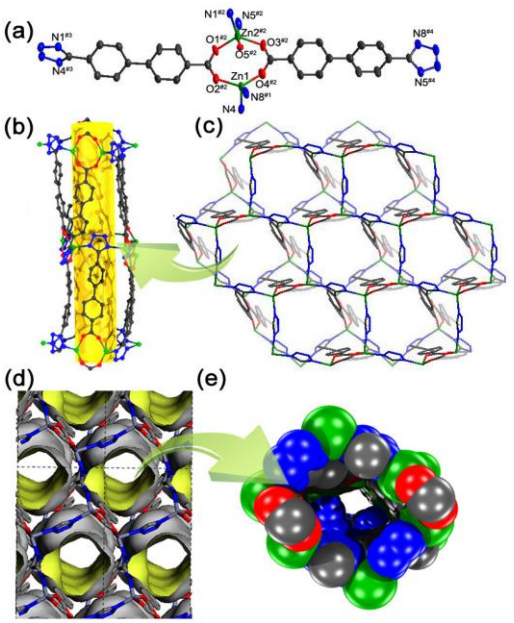

Fig. 1 The structure of **NENU-520**: (a) the coordination environments of Zn(II) atoms, symmetry codes:#1 0.5+x, 0.5+y, z; #2 1+x, y, z; #3 0.5+x, 1.5-y, 0.5+z; #4 x, 1-y, -0.5+z; (b) the 1D channel along the b axis; (c) 3D framework of **NENU-520** along the *c* axis; (d) the Connolly surface diagram displays the three dimensional irregular tunnels of **NENU-520**, and (e) the 1D channel in spacefilling mode along the c axis. All the hydrogen atoms are omitted for clarity.

The permanent porosity of **NENU-520** was unambiguously established by the N_2 sorption isotherm at 77 K. The activated samples **NENU-520a** were prepared by exchanging the solvent and characterized by thermal gravimetric analysis (TGA, Fig. S6) and PXRD patterns (Fig. S5), indicating the maintenance of the framework since the broadened peaks keep the positions. **NENU-520a** shows a characteristic type I behaviour with a BET surface area of 387 $m^2\ g^{-1}$ and a pore volume of 0.27 $cm^3\ g^{-1}$ based on the N_2 sorption isotherm (Fig. 2). The slight hysteresis between the adsorption and desorption profile perhaps can be explained by the 1D narrow channel system, which hints the escape of adsorbed gas molecules, as well as probably involving the structural breathing of the framework during the adsorption-desorption process.[37,38] Using the Horvath-Kawazoe (HK) method on the N_2 desorption isotherms,

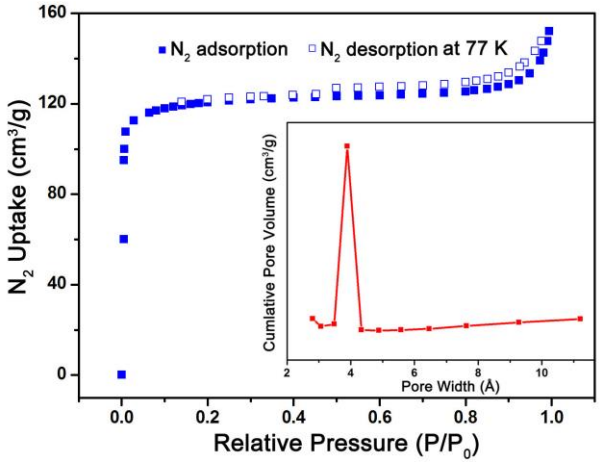

Fig. 2 The N_2 sorption isotherms at 77 K. Inset: the pore size distribution of **NENU-520a** using Horvath-Kawazoe (HK) method.

pore size distribution (Fig. 2) was estimated, which is basically identical to the measurement according to single-crystal X-ray diffraction study.

Low-pressure H_2 adsorption isotherms for **NENU-520a** were collected at 77 and 87 K, which is completely reversible, as shown in Fig. S7a. **NENU-520a** adsorbs 1.36 wt% of H_2 (152.4 cm^3 g^{-1} or 19.6 H_2 molecules per formula unit) at 77 K, and 1.09 wt% (121.6 cm^3 g^{-1} or 15.5 H_2 molecules per formula unit) at 87 K. It is indicative of the presence of strongly polarizing binding sites with a high affinity for H_2 from the steep initial portion of each isotherm. To gain further insights into H_2 adsorption, the behaviour of the isosteric heat was calculated using the Clausius–Clapeyron equation.[39] **NENU-520a** shows near–zero coverage Q_{st} value of 10.7 kJ mol^{-1} (Fig. S7b), which is compared with many famous porous materials, such as MOF-5 (7.6 kJ mol^{-1}), Zn-MOF-74 (8.3 kJ mol^{-1}), NOTT-101 (5.3 kJ mol^{-1}) and UMCM-150 (7.3 kJ mol^{-1}).[40,41] This result was attributed to the small pore diameter in **NENU-520a**, wherein overlapping potentials from two or more pore walls interact with a single H_2 molecule.[42,43] In addition, the uncoordinated N-heteroatom sites also aid in the low-pressure uptake by this material.[31]

Since accessible N-donor sites are expected to enhance interactions between frameworks and CO_2, the CO_2 sorption isotherms were measured at different temperatures, which shows a fully reversible type I behaviour with no hysteresis (Fig. 3). The CO_2 uptake of **NENU-520a** at saturation was 106.0 cm^3 cm^{-3} (corresponding to 15.7 wt % or 10.3 CO_2 per formula unit, Table S3) at 273 K and 79.9 cm^3 cm^{-3} (corresponding to 11.9 wt % or 7.8 CO_2 per formula unit) at 298 K. Albeit these values are lower than the M-MOF-74 series (162 cm^3 cm^{-3}) with different open metal sites, but much higher than lots of well-known MOFs, such as MAF-23 (or $Zn_2(btm)_2$, 74.2 cm^3 g^{-1} and 56.1 cm^3 g^{-1} at 273 K and 298 K) with multiple strong adsorption sites, $[Cu(tba)_2]_n$ (51.8 cm^3 g^{-1} or 10.2 wt % at 273 K), the currently best performing ZIF-69 (70 cm^3 g^{-1} at 273 K and 1 atm) and so on.[44-46] For practical use of an adsorptive material, the regeneration and recycling property

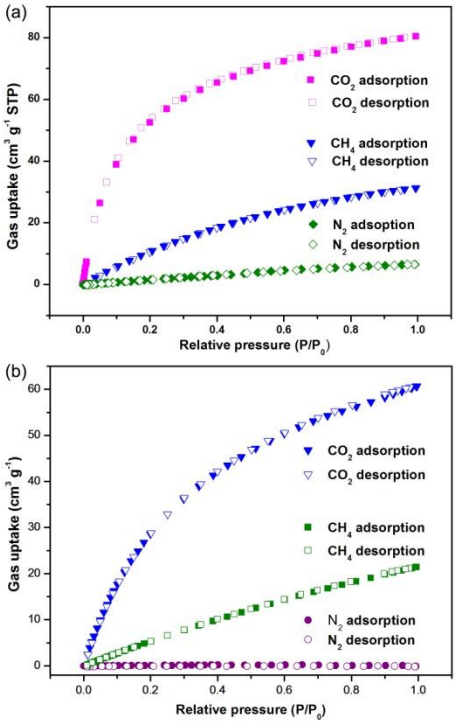

Fig. 3 The CO_2, CH_4 and N_2 sorption isotherms for **NENU-520a** at 273 K (a) and 298 K (b), respectively.

is crucial, which is also an important standard to evaluate an adsorption material. Keeping this in mind, the regenerative feature of **NENU-520a** was investigated. The powder X-ray diffraction pattern (Fig. S8) of **NENU-520a** after three cycles is in good agreement with that of the original structural characteristics, revealing its good stability. Moreover, **NENU-520a** basically maintains high adsorption capacity after three cycles of the regeneration experiment. This excellent behavior is significant for all MOFs analyzed, and the reproducibility demonstrates that uptake and release is nondestructive.

Sorption behaviours of **NENU-520a** toward CH_4 and N_2 were also studied at 273 and 298 K (Fig. 3). The desolvated **NENU-520a** only has a maximum CH_4 uptake of 31.3 cm^3 g^{-1} (1.4 mmol g^{-1}, 2.24 wt %) and 21.41 cm^3 g^{-1} (0.96 mmol g^{-1}, 1.53 wt %) at 273 and 298 K, which is substantially lower than CO_2. In sharp contrast to CO_2 and CH_4, the uptake of N_2 reaches a maximum of only 6.6 cm^3 g^{-1} (0.29 mmol g^{-1}) at 273 K and 0.23 cm^3 g^{-1} (0.01 mmol g^{-1}) at 298 K, respectively. It is clearly shown that the pore structure of **NENU-520a** is readily accessible to CO_2. The relatively high CO_2 and marginal N_2 uptake at ambient temperature prompted us to investigate the capacity of **NENU-520a** to selectively adsorb CO_2 over CH_4 and N_2.

The ideal adsorbed solution theory (IAST) calculation, originated by Myers and Prausnitz,[47] was employed to predict adsorption selectivity and CO_2 uptake of **NENU-520a** for the following binary gas mixtures: 15/85 CO_2/N_2, 50/50 CO_2/CH_4 and 5/95 CO_2/CH_4. The Langmuir-Freundlich equation fits extremely well with the single-component isotherms at 273 and

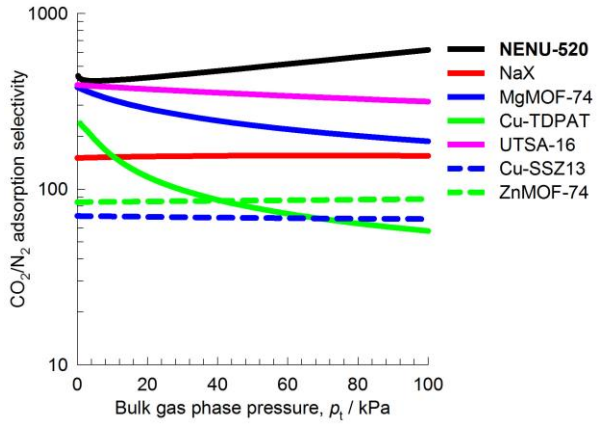

Fig. 4 Calculated selectivity of CO_2/N_2 predicted by IAST calculations 298 K for the variety of MOFs considered in this work. In these calculations, the partial pressures of CO_2 and CH_4 are taken to be p_1/p_2 = 15/85.

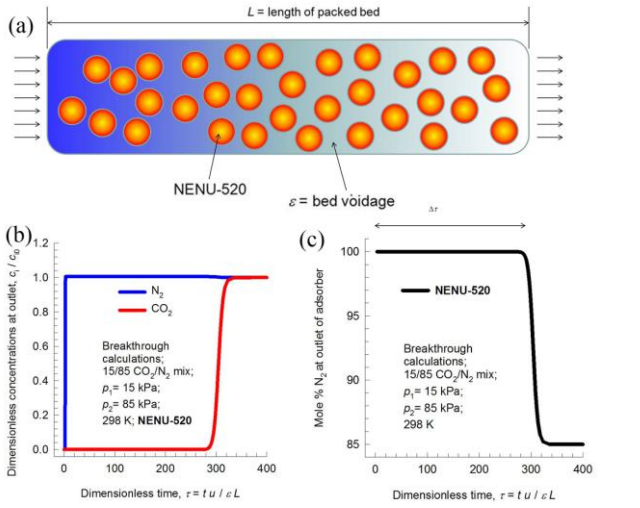

Fig. 5 (a) Schematic view of a packed bed adsorber. The tube length L = 0.3 m. The apparatus is operated at 298 K. The bed porosity, ε = 0.4. The interstitial gas velocity, u = 0.04 m/s; (b) breakthrough characteristics of an adsorber packed with **NENU-520** and maintained at isothermal conditions at 298 K, and (c) Mole percent N_2 in outlet gas as a function of the dimensionless time for operation at a total pressure of 100 kPa for 15/85 CO_2/N_2 mixture.

298 K (Fig. S9), and the fitting parameters were listed in Table S4. Evaluation of the selectivity of adsorbents at atmospheric pressure for the CO_2−N_2 mixture was essential for a realistic post-combustion capture of CO_2. In these calculations, the partial pressures of CO_2 and N_2 are taken to be 15 kPa and 85 kPa, respectively. For comparison, six representative MOFs or zeolites (NaX, MgMOF-74, Cu-TDPAT, UTSA-16, Cu-SSZ13 and ZnMOF-74)[35,36] exhibiting high CO_2/N_2 separation selectivity are also included. Fig. 4 presents the IAST calculations for CO_2/N_2 adsorption selectivity. Remarkably, **NENU-520** has the highest selectivity (about 400) towards CO_2 for mixture compositions. To the best of our knowledge, only two MOFs were reported displaying higher CO_2/N_2 selectivity than **NENU-520**. One example is the SIFSIX-3-Zn, which exhibits the highest CO_2/N_2 selectivity (with selectivity of 1539±307).[28] During the course of this work, SIFSIX-3-Zn has more-regular square-shaped channels with dimensions of 3.84 Å and lined with Lewis basic groups on the SiF_6 anions that notably enhance the uptake of CO_2 into the material. While, neither charged units nor favourable groups are existed in the channels of **NENU-520**. The other is [Cu(bcppm)H_2O]. Although [Cu(bcppm)H_2O] has somewhat higher selectivity, its uptake capacity (1.70 and 1.85 mmol g^{-1} at 293 and 273 K, respectively) is apparently lower than **NENU-520** (2.71 and 3.59 mmol g^{-1} at 298 and 273 K, respectively).[36] The selectivity is obviously superior to most of MOFs and ranks **NENU-520** among the highest selectivity values (Table S5) with the absence of unsaturated metal centres, charged units and amine groups.[46,48-57] Importantly, **NENU-520** is one of best materials to facilitate effective CO_2 capture and separation from the perspective of comprehensive properties.

The selectivities for CO_2/CH_4 were also evaluated when the gas phase compositions are 5/95 and 50/50 (Fig. S10), and the corresponding values are comparable to most MOFs reported in the literatures, although it has a lower selectivity than Mg-MOF-74.

In view of the feasibility for separation performance of **NENU-520**, transient breakthrough simulations using the methodology described in the literature was performed.[58-64] The performance of industrial fixed bed adsorbers is dictated by a combination of adsorption selectivity and uptake capacity. The proper combination of both of these factors is obtained by use of breakthrough calculations. Fig. 5a shows a schematic of a packed bed adsorber. The x axis in Fig. 5b and c is a dimensionless time, τ, defined by dividing the actual time, t, by the characteristic times, $L\varepsilon/u$. Longer breakthrough time is desirable from a practical point of view because this implies a less frequent requirement for regeneration. Figure 5b presents the breakthrough characteristic as a function of the dimensionless time in an adsorber packed with **NENU-520a** at a total pressure of 100 kPa for 15/85 CO_2/N_2 mixture, which represents conditions relevant for flue gas processing. For **NENU-520a**, the sequence of breakthroughs is dictated by the adsorption strengths, the more strongly adsorbing CO_2 elutes last in the sequence. Fig. 5c presents the mole percent of N_2 in outlet gas as a function of the dimensionless time with **NENU-520a**. It is possible to recover pure N_2 from the gas mixture in a certain interval of time. We arbitrarily set the purity requirement to be 99.95% N_2. This amount can be determined from a material balance. The productivity of N_2 with a purity of 99.95%+ can be determined to be 4.84 mol kg^{-1} of **NENU-520**. The reason for the high productivity is a combination of higher selectivity and higher CO_2 uptake capacity. **NENU-520a** was demonstrated to be a promising candidate for CO_2 capture and separation from fuel gas.

5/95 CO_2/CH_4 mixture breakthrough characteristics as a function of the dimensionless time in an adsorber packed (as shown in Fig. S11). **NENU-520a** outperforms longer breakthrough time than ZIF-78 (81), UTSA-20a (86), MIL-101 (32) and so on.[28] In natural gas purification processes, the

primary objective is to produce CH_4 with a specified purity level, which is typically 500 ppm CO_2, i.e. 0.05 mole percent CO_2. Fig. S11b shows the gas composition, expressed as mole percent of CH_4 in outlet gas as a function of the dimensionless time for a selection of porous adsorbent materials. During the time interval $\Delta\tau$, 99.95%+ pure CH_4 can be produced. The productivity of methane with a purity of 99.95%+ is calculated to be 6.7 mol kg^{-1} of **NENU-520** determined from the material balance on the fixed bed adsorber. In addition, the composition of natural gas changes frequently. The breakthrough characteristics for binary 50/50 mixture of CO_2 and CH_4 are also presented (Fig. S12). The breakthrough occurs at a shorter dimensionless time than for 5/95 binary mixture. And the productivity is 1.79 mol per kg of **NENU-520** during the time interval $\Delta\tau$. The results from these studies all confirm **NENU-520** has the ability to separate N_2 and CH_4 in pure form from gas mixtures. Based on the presented evidence, **NENU-520** is a superior adsorbent for CO_2/N_2 and CO_2/CH_4 separation at ambient conditions than reported for most MOFs.

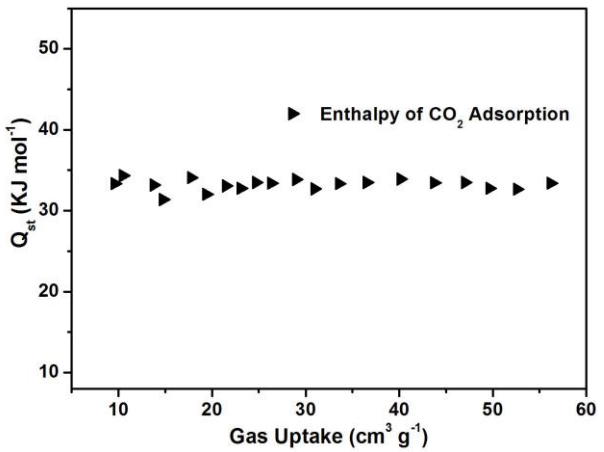

Fig. 6 Heats of CO_2 adsorption as a function of CO_2 uptake for **NENU-520**.

The CO_2 adsorption enthalpy of **NENU-520a** is 33 kJ mol^{-1} (Fig. 6), which is stronger than siliceous zeolite (27 kJ mol^{-1}), and series of MAF materials (MAF-4, 25.1 kJ mol^{-1}; MAF-7, 17.2 kJ mol^{-1}; MAF-25, 26.3 kJ mol^{-1} and MAF-26, 23.3 kJ mol^{-1}; MAF stands for metal azolate framework).[30,65,66] The CH_4 adsorption enthalpy is 29 kJ mol^{-1}. The high uptake and enthalpy of CO_2 as well as the remarkable selectivity over CH_4 and N_2 may be reasonable considering the fact that: (i) with its greater polarizability and larger quadrupole moment, CO_2 has stronger interactions with the accessible N-sites of **NENU-520** than do CH_4 and N_2;[67-69] (ii) the abundant uncoordinated N-heteroatom sites directing toward the inner surface in the narrow cavities are beneficial to interact with CO_2 molecules; (iii) As mentioned above, the kinetic diameters of the cylinders are 3.3 Å 3.64 Å and 3.80 Å for CO_2, N_2 and CH_4, respectively. The limiting pore size (about 3.6 Å) of **NENU-520** is just right for CO_2. Thus, CO_2 molecules are more prone to be injected than CH_4 and N_2.

Inspired by the reported charge transfer electron transitions between the microporous MOFs and the guest molecules, the potential luminescent sensitivity and selectivity of **NENU-520** was also investigated in different organic solvents, such as cyclohexane, toluene, acetonitrile, benzene, chloroform, *p*-xylene, *n*-hexane, *m*-xylene, THF and nitrobenzene. The results suggest that the emission intensities are largely dependent on different solvent molecules (Fig. S13a and b). Moreover, the obvious quenching phenomenon for nitrobenzene was examined in detail (See Supplementary Information). As shown in Fig. S13c and d, **NENU-520** can sensitively detect a very small amount of nitrobenzene (30 ppm in DMF) through noticeable fluorescence decay, demonstrating extremely high sensitivity towards nitrobenzene. Until now, several MOF-based fluorescent sensors have been developed for the detection of nitroaromatic explosives.[70,71] The intensity of **NENU-520** was nearly completely quenched at a concentration of 100 ppm with a high quenching efficiency of 96.6%, which is higher than other MOF sensors toward nitrobenzene.[72] In addition, **NENU-520** can be regenerated for recycling by centrifuging solution after use and then washing several times with DMF. The quenching efficiencies of cycle 1−4 were not decreased (100 ppm), displaying high recyclability and stability in detection application (Fig. S14, S15 and S16), which is favourable for its potential application of detecting explosives containing nitrobenzene molecules. Referring to the reported works, **NENU-520** is presumably attributed to not only the good dispersible nature of MOF particles but also the electron deficient nature of nitrobenzene and the high electron rich conjugated framework structure.[70,71]

Conclusions

In conclusion, a new N-rich MOF has been successfully harvested by means of solvothermal reaction. **NENU-520** has good air-stability even in the existence of moisture. Activated **NENU-520a** exhibits strong adsorption capacity towards H_2 and CO_2 with high adsorption enthalpy of 10.7 kJ mol^{-1} and 33 kJ mol^{-1}, respectively. Moreover, **NENU-520a** shows high CO_2/CH_4 and CO_2/N_2 selectivities calculated *via* combination of the Ideal Adsorbed Solution Theory and breakthrough simulations for a realistic consideration. In particular, the selectivity of CO_2 over N_2 at 298 K of **NENU-520a** is amongst the highest values for CO_2 selective separation. Consequently, **NENU-520a** has significant potential for use as adsorbent in CO_2-capture for natural gas sweetening and post-combustion power plants, combines the higher uptake and higher selectivity toward CO_2. The narrow but suitable channel as well as the effective accessible nitrogen donors directing toward the inner surface is demonstrated to be the predominant factor for the high uptake capacity and unprecedented selectivity. Additionally, **NENU-520a** displays highly selective, sensitive and recyclable properties in detection of nitrobenzene as a fluorescent sensor because of its quenching effect in nitrobenzene.

Acknowledgements

This work was financially supported by Pre-973 Program (No. 2010CB635114), the National Natural Science Foundation of China (No. 21371099, 21471080 and 21401021), the Science and Technology Development Planning of Jilin Province (No. 20140203006GX and 20140520089JH), the Fundamental Research Funds for the Central Universities (No. 14QNJJ013), the Jiangsu Specially-Appointed Professor, the NSF of Jiangsu Province of China (No. BK20130043), the Natural Science Research of Jiangsu Higher Education Institutions of China (No. 13KJB150021), the Priority Academic Program Development of Jiangsu Higher Education Institutions and the Foundation of Jiangsu Collaborative Innovation Center of Biomedical Functional Materials.

Notes and references

[a] Institute of Functional Material Chemistry, Faculty of Chemistry, Northeast Normal University, Changchun 130024 Jilin, P. R. China. Email: zmsu@nenu.edu.cn.

[b] Jiangsu Key Laboratory of Biofunctional Materials, School of Chemistry and Materials Science, Nanjing Normal University, Nanjing 210023 Jiangsu, P. R. China. E-mail: yqlan@njnu.edu.cn.

[c] Van't Hoff Institute for Molecular Sciences, University of Amsterdam Science Park 904, 1098 XH Amsterdam (The Netherlands).

[d] College of Chemistry and Life Sciences, Zhejiang Normal University, Jinhua 321004 Zhejiang, China.

† Electronic Supplementary Information (ESI) available: Experimental details, PXRD patterns, TGA, IR curves, crystallographic data, additional figures, IAST and breakthrough calculations for **NENU-520**. CCDC: 990058. For ESI and crystallographic data in CIF or other electronic format see DOI: 10.1039/b000000x/

1 J. R. Li, J. Sculley and H. C. Zhou, *Chem. Rev.*, 2012, **112**, 869.
2 D. M. D'Alessandro, B. Smit and J. R. Long, *Angew. Chem. Int. Ed.*, 2010, **49**, 6058.
3 M. Z. Jacobson, *Energy Environ. Sci.*, 2009, **2**, 148.
4 K. M. K. Yu, I. Curcic, J. Gabriel and S. C. E. Tsang, *ChemSusChem*, 2008, **1**, 893.
5 G. Petron, P. Tans, G. Frost, D. Chao and M. Trainer, *J. Geophys. Res.*, 2008, **113**, 1.
6 S. Solomon, G. K. Plattnera, R. Knutti and P. Friedlingstein, *Proc. Natl. Acad. Sci. U.S.A.*, 2009, **106**, 1704.
7 N. MacDowell, N. Florin, A. Buchard, J. Hallett, A. Galindo, G. Jackson, C. S. Adjiman, C. K. Williams, N. Shah and P. Fennell, *Energy Environ. Sci.*, 2010, **3**, 1645.
8 E. D. Bloch, L. J. Murray, W. L. Queen, S. Chavan, S. N. Maximoff, J. P. Bigi, R. Krishna, V. K. Peterson, F. Grandjean, G. J. Long, B. Smit, S. Bordiga, C. M. Brown and J. R. Long, *J. Am. Chem. Soc.*, 2011 , **133**, 14814.
9 S. Chaemchuen, N. A. Kabir, K. Zhou, F. Verpoort, *Chem. Soc. Rev.*, 2013, **42**, 9304.
10 J. Wang, L. Huang, R. Yang, Z. Zhang, J. Wu, Y. Gao, Q. Wang, D. O'Hare and Z. Zhong, *Energy Environ. Sci.*, 2014, DOI: 10.1039/c4ee01647e.
11 R. Service, *Science*, 2004, **305**, 962.
12 B. A. Peppley, *Int. J. Green Energy*, 2006, **3**, 195.
13 N. Muradov, *Int. J. Hydrogen Energy*, 2001, **26**, 1165.
14 H.-L. Jiang, D. Feng, K. Wang, Z.-Y. Gu, Z. Wei, Y.-P. Chen and H.-C. Zhou, *J. Am. Chem. Soc*., 2013, **135**, 13934.
15 Z. Yin, Q. X. Wang and M. H. Zeng, *J. Am. Chem. Soc.*, 2012, **134**, 4857.
16 Y. He, W. Zhou, R. Krishna and B. Chen, *Chem. Commun.*, 2012, **48**, 11813.
17 Y. Q. Lan, H. L. Jiang, S. L. Li and Q. Xu, *Adv. Mater.*, 2011, **23**, 5015.
18 F. Akhtar, Q. Liu, N. Hedin and L. Bergström, *Energy Environ. Sci.*, 2012, **5**, 7664.
19 J. B. DeCoste, G. W. Peterson, *Chem. Rev.*, 2014, **114**, 5727.
20 Y. He, B. Li, M. O'Keeffe and B. Chen, *Chem. Soc. Rev.*, 2014, **43**, 5618.
21 Z. Zhang, Y. Zhao, Q. Gong, Z. Li and J. Li, *Chem. Commun.*, 2013, **49**, 653.
22 J. R. Li, R. J. Kuppler and H. C. Zhou, *Chem. Soc. Rev.*, 2009, **38**, 1477.
23 S. Couck, J. F. M. Denayer, G. V. Baron, T. Remy, J. Gascon and F. Kapteijn, *J. Am. Chem. Soc.*, 2009, **131**, 6326.
24 R. Vaidhyanathan, S. S. Iremonger, G. K. H. Shimizu, P. G. Boyd, S. Alavi and T. K. Woo, *Angew. Chem. Int. Ed.*, 2012, **51**, 1826.
25 J. L. C. Rowsell and O. M. Yaghi, *Angew. Chem. Int. Ed.*, 2005, **44**, 4670.
26 B. Zheng, Z. Yang, J. Bai, Y. Li and S. Li, *Chem. Commun.*, 2012, **48**, 7025.
27 Y. Wang, C. Tan, Z. Sun, Z. Xue, Q. Zhu, C. Shen, Y. Wen, S. Hu, Y. Wang, T. Sheng and X. Wu, *Chem. Eur. J.*, 2014, **20**, 1341.
28 P. Nugent, Y. Belmabkhout, S. D. Burd, A. J. Cairns, R. Luebke, K. Forrest, T. Pham, S. Ma, B. Space, L. Wojtas, M. Eddaoudi and M. J. Zaworotko, *Nature*, 2013, **495**, 80.
29 J. M. Taylor, K. W. Dawson and G. K. H. Shimizu, *J. Am. Chem. Soc.*, 2013, **135**, 1193.
30 J. P. Z, J. B. Lin and X. M. Chen, *J. Am. Chem. Soc.*, 2010, **132**, 6654.
31 J. S. Qin, D. Y. Du, W. L. Li, J. P. Zhang, S. L. Li, Z. M. Su, X. L. Wang, Q. Xu, K. Z. Shao and Y. Q. Lan, *Chem. Sci.*, 2012, **3**, 2114.
32 P. Cui, Y. G. Ma, H. H. Li, B. Zhao, J. R. Li, P. Cheng, P. B. Balbuena and H. C. Zhou, *J. Am. Chem. Soc.*, 2012, **134**, 18892.
33 Q. Lin, T. Wu, S. T. Zheng, X. Bu and P. Feng, *J. Am. Chem. Soc.*, 2012, **134**, 784.
34 A. L. Spek, J. Appl. Crystallogr., 2003, **36**, 7.
35 S. Xiang, Y. He, Z. Zhang, H. Wu, W. Zhou, R. Krishna and B. Chen, *Nat. Commun.*, 2012, **3**, 954.
36 W. M. Bloch, R. Babarao, M. R. Hill, C. J. Doonan and C. J. Sumby, *J. Am. Chem. Soc.*, 2013, **135**, 10441.
37 S. Xiang, J. Huang, L. Li, J. Zhang, L. Jiang, X. J. Kuang and C.-Y. Su, *Inorg. Chem.*, 2011, **50**, 1743.
38 L. Hou, L. N. Jia, W. J. Shi, Y. Y. Wang, B. Liu and Q. Z. Shi, *Dalton Trans.*, 2013, **42**, 3653.
39 S. S. Kaye and J. R. Long, *J. Am. Chem. Soc.*, 2005, **127**, 6506.
40 M. P. Suh, H. J. Park, T. K. Prasad and D. W. Lim, *Chem. Rev.*, 2012, **112**, 782.
41 R. B. Lin, D. Chen, Y. Y. Lin, J. P. Zhang and X. M. Chen, *Inorg. Chem.*, 2012, **51**, 9950.

42 M. Dincă, A. Dailly, Y. Liu, C. M. Brown, D. A. Neumann and J. R. Long, *J. Am. Chem. Soc.*, 2006, **128**, 16876.
43 S. L. Li and Q. Xu, *Energy Environ. Sci.*, 2013, **6**, 1656.
44 J. Duan, M. Higuchi, R. Krishna, T. Kiyonaga, Y. Tsutsumi, Y. Sato, Y. Kubota, M. Takata and S. Kitagawa, *Chem. Sci.*, 2014, **5**, 660.
45 P. Q. Liao, D. D. Zhou, A. X. Zhu, L. Jiang, R. B. Lin, J. P. Zhang and X. M. Chen, *J. Am. Chem. Soc.*, 2012, **134**, 17380.
46 M. Du, C. P. Li, M. Chen, Z. W. Ge, X. Wang, L. Wang and C. S. Liu, *J. Am. Chem. Soc.*, 2014, **136**, 10906.
47 A. L. Myers and J. M. Prausnitz, *AIChE J.*, 1965, **11**, 121.
48 B. Zheng, J. Bai, J. Duan, L. Wojtas and M. J. Zaworotko, *J. Am. Chem. Soc.*, 2011, **133**, 748.
49 M. Zhang, Q. Wang, Z. Lu, H. Liu, W. Liu and J. Bai, *CrystEngComm*, 2014, **16**, 6287.
50 A. K. Sekizkardes, T. İslamoğlu, Z. Kahveci and H. M. El-Kaderi, *J. Mater. Chem. A*, 2014, **2**, 12492.
51 T. M. McDonald, W. R. Lee, J. A. Mason, B. M. Wiers, C. S. Hong and J. R. Long, *J. Am. Chem. Soc.*, 2012, **134**, 7056.
52 X. Lv, L. Li, S. Tang, C. Wang and X. Zhao, *Chem. Commun.*, 2014, **50**, 6886.
53 Y. Liu, S. Wu, G. Wang, G. Yu, J. Guan, C. Pan and Z. Wang, *J. Mater. Chem. A*, 2014, **2**, 7795.
54 R.-J. Li, M. Li, X.-P. Zhou, S. W. Ng, M. O'Keeffe and D. Li, *CrystEngComm*, 2014, **16**, 6291.
55 L. Du, Z. Lu, K. Zheng, J. Wang, X. Zheng, Y. Pan, X. You and J. Bai, *J. Am. Chem. Soc.*, 2013, **135**, 562.
56 J. B. L. and G. K. H. Shimizu, *Inorg. Chem. Front.*, 2014, **1**, 302.
57 T. M. McDonald, D. M. D'Alessandro, R. Krishna and J. R. Long, *Chem. Sci.*, 2011, **2**, 2022.
58 R. Krishna and J. R. Long, *J. Phys. Chem. C*, 2011, **115**, 12941.
59 R. Krishna, *Microporous Mesoporous Mater.*, 2014, **185**, 30.
60 D. L. Chen, H. Shang, W. Zhu and R. Krishna, *Chem. Eng. Sci.*, 2014, **117**, 407.
61 D. L. Chen, N. Wang, F. F. Wang, J. Xie, Y. Zhong, W. Zhu, J. K. Johnson and R. Krishna, *J. Phys. Chem. C*, 2014, **118**, 17831.
62 H. H. Wu, K. X. Yao, Y. H. Zhu, B. Y. Li, Z. Shi, R. Krishna and J. Li, *J. Phys. Chem. C*, 2012, **116**, 16609.
63 C. Song, Y. He, B. Li, Y. Ling, H. Wang, Y. Feng, R. Krishna and B. Chen, *Chem. Commun.*, 2014, **50**, 12105.
64 J. J. Perry, S. L. TeichMcGoldrick, S. T. Meek, J. A. Greathouse, M. Haranczyk and M. D. Allendorf, *J. Phys. Chem. C*, 2014, **118**, 11685.
65 Z. Zhang, Z. Z. Yao, S. Xiang and B. Chen, *Energy Environ. Sci.*, 2014, **7**, 2868.
66 R. Dawson, E. Stockel, J. R. Holst, D. J. Adams and A. I. Cooper, *Energy Environ. Sci.*, 2011, **4**, 4239.
67 K. Sumida, D. L. Rogow, J. A. Mason, T. M. McDonald, E. D. Bloch, Z. R. Herm, T.-H. Bae and J. R. Long, *Chem. Rev.*, 2012, **112**, 724.
68 Y.-S. Bae and C. H. Lee, *Carbon*, 2005, **43**, 95.
69 S. R. Caskey, A. G. Wong-Foy and A. J. Matzger, *J. Am. Chem. Soc.*, 2008, **130**, 10870.
70 H. Xu, F. Liu, Y. Cui, B. Chen and G. Qian, *Chem. Commun.*, 2011, **47**, 3153.
71 M. Guo and Z.-M. Sun, *J. Mater. Chem.*, 2012, **22**, 15939.
72 D. Tian, Y. Li, R.-Y. Chen, Z. Chang, G. Wang and X. H. Bu, *J. Mater. Chem. A*, 2014, **2**, 1465.